Statistics of scattering backgrounds in threshold images

B.D. Borisov

Institute of Atmospheric Optics,
Siberian Branch of the Russian Academy of Sciences, Tomsk

Received April 17, 2007

The structure of scattering backgrounds in optical imaging of low-intensity objects through smoke layers of different optical densities is considered.

The most complete information about an object can be obtained from an optical signal by taking into account spatiotemporal photon distributions.[1] To optimize construction of the corresponding structure schemes for recording images of low-reflecting and low-emitting objects, as well as to optimize operation of systems detecting optical information under unfavorable optical and weather conditions, the study of spatiotemporal statistics of a signal and a background in the image plane are needed. This is required in the problems of synthesis of threshold images, when using multichannel detectors with limiting sensitivity characteristics. The spatiotemporal statistics of photocounts of the scattered radiation field also carries additional information about properties of the medium.[2]

This paper describes experiments on estimation of some characteristics of backgrounds appearing during synthesis of images of a small-size nonstationarily emitting diffuse object of extremely low brightness in the case of radiation propagation through a scattering medium of different optical density.

The experiments were conducted in the Big Aerosol Chamber of the Institute of Atmospheric Optics. The chamber's volume is 1780 m^3. A low-absorbing scattering medium was produced in the process of the wood thermal decomposition without direct access of oxygen (smoke generation by pyrolysis). The characteristics of such media are considered in detail in Ref. 3.

The simplified block diagram of the experiment is shown in Fig. 1.

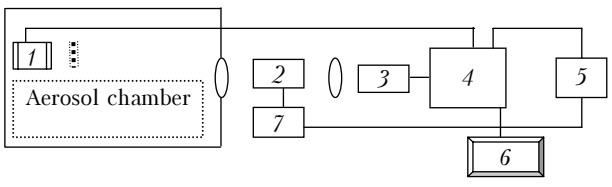

Fig. 1. Block diagram of the experimental setup: semiconductor laser with an opal plate *1*; image intensifier tube with a receiving objective *2*; TV camera with image transfer optics *3*; radio channel module of the TV system *4*; adjustable delay module *5*; monitor *6*; gate-pulse generator *7*.

The experimental setup consisted of two measurement systems. The first system, served for accompanying measurements of the optical density, was a photometer with reflection, including a He–Ne laser ($\lambda = 0.63$ μm) and two channels for measurement of the reference and information signals. The second measurement system consisted of a receiving objective and an image intensifier with pulsed supply of a microchannel plate, which served as a fast-acting gate. Due to high amplification coefficient of light flux in this system, we succeeded in detection of individual photons. Scintillations from the image intensifier monitor were recorded with a high-sensitivity TV camera tube.[4] Then the TV signal came directly to the input of the video converter of a personal computer or to an intermediate magnetic carrier.

The radiation source was represented by a semiconductor laser with a band of 0.89–0.93 μm and a pulse duration at a half-width of 150 ns. An opal glass plate bounded by a diaphragm of 10 mm in diameter was installed in front of the laser. The glass converted the laser radiation into the diffuse light flux with a direction pattern of larger than 100°.

The measurement system operated as follows. Simultaneously with the laser triggering, a frame-synchronizing pulse of the radio channel module of the TV system *4* started, after the adjustable delay *5*, the gate-pulse generator *7*, which generated the pulsed voltage across the microchannel plate of the image intensifier with an amplitude of 900 V and a duration of 150 ns. Using the delay, the gate pulse was set at any time interval relative to the laser pulse accurate to 20 ns.

On the whole, the setup configuration allowed imitation (with some assumptions) of the action of an active observation system with a cutoff of the backscattering noise or to model in optical information systems the pulsed spatial signal transfer through scattering media.

To keep the receiving system in the photon-counting mode, neutral filters were used or the adaptation into the counting mode was performed by the gate pulse temporal shift relative to the incoming laser pulse.

The recording of one realization in the measurement system by the given recording method (for example, the installed neutral filter and the

0235-6880/07/10 783-04 $02.00

absolute temporal coincidence of the laser and gate pulses) took more than a half of an hour. For this time, the medium optical thickness, permanently monitored, decreases by 6–8% relative to the initial one.

Samples of duration $T \approx 16$ min with readouts every 2.4 s, that is, containing 400 spatiotemporal readouts (frames) were inputted into the personal computer. The mathematical processing consisted in calculation of the spatiotemporal distribution of photocounts in the observation system. For this purpose, after accumulation of photocounts and their frame-by-frame summation, the coordinates and the size of the probed area in the plane of the source image were determined. Each photocount, recorded on the probed area, was computer-analyzed for the absence of intersections with other photocounts. In case of "adhesion" of photocounts, only a single value was taken into consideration.

The distribution function $P(n, T)$ was determined as an empirical frequency of appearance of n_i photocounts in a TV frame (T is the time of accumulation).

In the image plane of the observation system used, the source image occupied an area of about 30×30 pixels (angular dimensions of the observed object were about 1.3 mrad). In the processing of the experimental material, the probed area was taken equal to 80×80 pixels ($\approx 3 \times 3$ mrad in the field of view of the receiving system). The total field of view, in which photocounts of the forward scattered and direct radiation were recorded, was $\approx 15 \times 14$ mrad (413×382 pixels).

The photocount distribution functions (PHDFs) were analyzed for three spatial positions of the probed area in the field of view of the receiving system at different densities of the smoke aerosol along the observation path. In the first processing zone, the center of the probed area coincided with the image center, in the second zone it was shifted by 80 pixels toward the background, and at the third position the center was shifted by 200 pixels relative to the center of the source image. In the angular measure, this covered an area ≈ 8.6 mrad (about 0.5° of a half-angle). Thus, we studied processes proceeding in small scattering angles. Varying the time delay, we determined PHDFs for shorter recording (sampling) time T_0 than the time interval determined by the duration of the gate pulse.

When the probed area lied in the region of formation of the object image (signal) (the luminous opal glass plate bounded by the diaphragm in this case), the processing sphere included photocounts caused by the scattered radiation of the image vicinity. As a result, PHDF was the distribution resulted from the mixture of the signal and the scattering noise. The distribution of the signal mixed with the noise for equal mean values of photocounts and two separated optical thicknesses τ is shown in Fig. 2*a*.

The distribution curves, at first glance, looked similarly to the Poisson statistical model, but the analysis of the experimental material by the goodness criterion χ^2 has shown that all PHDF sets for all measured smoke aerosol thicknesses ($\tau = 0.25$–5.62) do not agree with this model. As well, the field of the source radiation recorded in the chamber free of smoke does not obey this distribution.

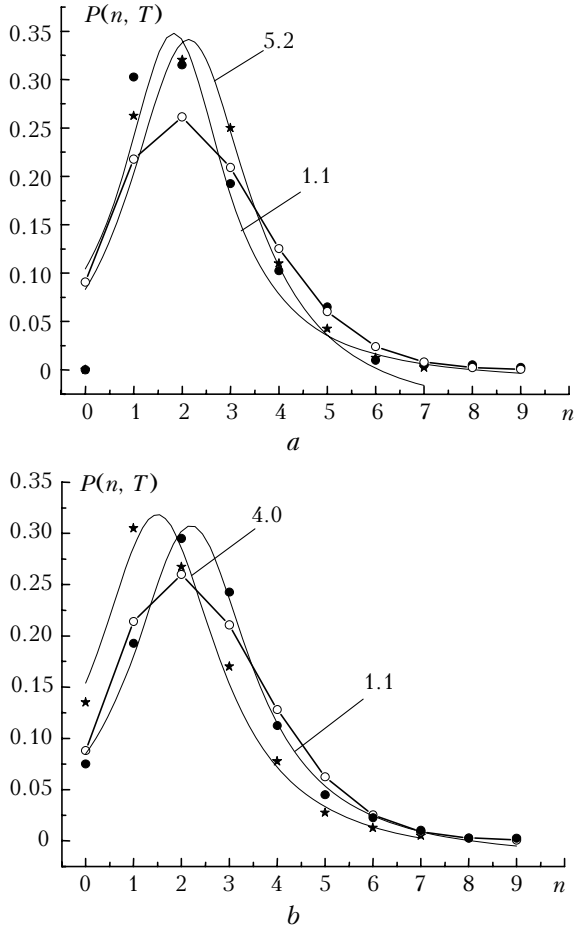

Fig. 2. Photocount distribution functions in the image plane of the receiving system: (*a*) distribution in the source image zone (first zone) for two values of the optical thickness τ (the values of τ are indicated near curves), experimental average values of photocounts $\langle n \rangle = 2.4$, calculation by the Poisson distribution formula for $\langle n \rangle = 2.4$ (open circles); (*b*) distributions in the background area (second zone, designations are the same, $\langle n \rangle = 2.0$–2.4, calculation for $\langle n \rangle = 2.4$.

The PHDF shape in the region of background adjacent to the area occupied by the source image is shown in Fig. 2*b*. The dependences are also shown for two spaced optical thicknesses with the close average values of photocounts.

As is well-known, the brightness of the forward scattered radiation in hazes for narrow steady-state light fluxes near the axis changes nonmonotonically with the τ increase. It is well described by single-scattering equations up to $\tau \approx 16$ [Ref. 5]. It is believed that the single scattering plays the primary role in formation of the background component of the forward scattered radiation in the smoke aerosol

under given experimental conditions. As an example, Fig. 3 shows the dependence of the forward-scattered radiation background intensity for the second conditional zone in the field of view of the receiving system on the medium optical thickness.

The intensities of the scattered radiation have been determined by taking into account the attenuation coefficients of the filters in the measured average values of photocounts. Figure 3 demonstrates that the background intensity changes nonmonotonically with the increasing optical thickness and has a peak near $\tau \approx 1$.

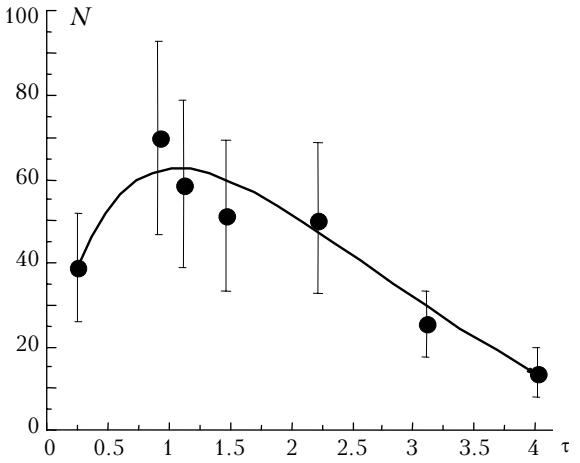

Fig. 3. Intensity N of background of the forward scattered radiation as a function of the medium optical thickness (second zone).

The evolution of the PHDF shape as a function of the position of the probed area in the image plane of the receiving system at a fixed τ can be seen in Fig. 4. It follows from the figure that as the probed area displaces from the object image toward the background, the character of background distributions changes.

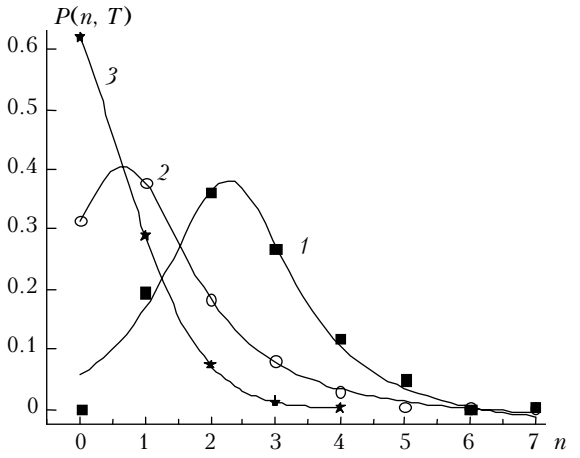

Fig. 4. Example of evolution of photocount distribution functions in the image plane of the receiving system, digits near curves are numbers of measurement zones, $\tau \approx 3.1$, average values of photocounts: (*1*) $\langle n \rangle = 2.56$, (*2*) 1.17, and (*3*) 0.2.

Possible cause for the change in the shape of the distribution curves is the dependences between the source coherence time $\tau_c \approx 1/\Delta\nu$, where $\Delta\nu$ is the band width, the recording time T_o, and the time stretching of the optical pulse caused by the scattering medium.

It is known that PHDFs can be described by particular statistical models in two limiting cases connected with the coherence time of a process and the recording time. The photon distribution for the constant intensity or for a chaotic source, when the condition $T_o \gg \tau_c$ is fulfilled, is described by the Poisson statistical model. At $T_o \ll \tau_c$, the photocount distribution of a chaotic source becomes simpler and is called the Bose–Einstein distribution.[2]

The distributions in the image and background regions in adjacent zones are close in shape, but the models of the distributions are not determined. In the third zone, the graphical analysis and estimates by the goodness criterion χ^2 have shown that PHDFs are well described by the Bose–Einstein statistical model in the entire range of the measured optical thicknesses. An example of the distribution is shown in Fig. 5*a*.

This form of the distribution at the periphery of the processed area can be explained by the combination of factors, which lead to $T_o \ll \tau_c$. Since the system began to operate as a multichannel photon counter at the maximal amplitude of the gate pulse generator, the real time of photon counting was determined not by the total pulse duration, but the duration of the pulse top part, and it was about 40 ns. The source coherence time calculated according to its rated band width was equal roughly to 70 ns. Since the resultant coherence time is determined by the field of the scattered light, whose coherence time is an order of magnitude larger than that of the source used in the experiment,[2] the condition $T_o \ll \tau_c$ is fulfilled. One more cause lies in the fact that as the distance from the image area increases, the higher orders of scattering contribute to the formation of the background.[5] The increase of the order of scattering may lead to a delay in arrival of photons into the recording zone and the corresponding decrease of T_o [Ref. 6].

As to the second zone, a possible cause for nonfulfillment of the inequality $T_o \ll \tau_c$ is the decisive influence of the single scattering in the background component. Since PHDF of the source does not correspond to the Poisson model, we can suppose that the source radiation is chaotic and the scattered radiation in the regions adjacent to the image strongly depends on the properties of the source radiation with similar temporal characteristics. In this case, the coherence time of the scattered light is close to the coherence time of the source. Then none of the threshold inequalities is fulfilled, and the PHDF approximation is determined for every particular case.

Varying the time position of the gate pulse relative to the source pulse allows creation of conditions close to $T_o \ll \tau_c$ for backgrounds of the

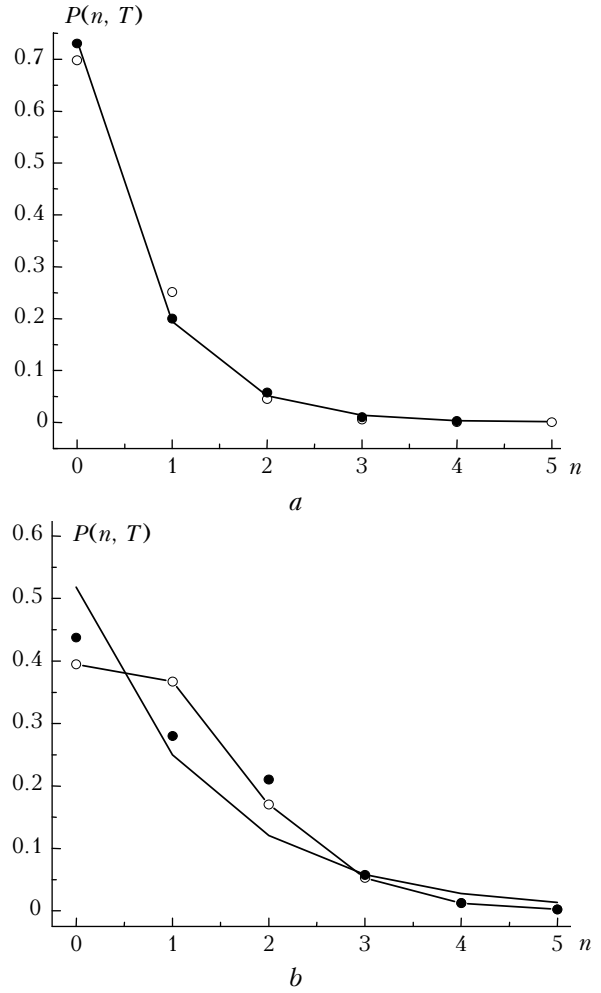

Fig. 5. Examples of photocount distribution functions in the image plane of the receiving system: (*a*) distribution in the background area (third zone), experiment (dots), calculation by the Bose–Einstein distribution (solid curve), calculation by the Poisson distribution (circles), $\tau \approx 4.0$, average value of photocounts $\langle n \rangle = 0.36$; (*b*) distribution in the background area obtained through the time shift of the gate pulse relative to the source pulse (second zone), designations are the same, $\tau \approx 4.6$, $\langle n \rangle = 0.93$.

second conditional zone directly adjacent to the image area. For example, this could be accomplished by covering the trailing edge of the source pulse by the leading edge of the gate pulse. In this case, delayed photons are recorded and T_o can be much shorter than the coherence time of the scattered light. The distribution obtained through the shift of the gate pulse is exemplified in Fig. 5*b*.

The analysis of the measurements allows us to note the following. The distribution parameters weakly depend on variations of the optical thickness of the wood smoke aerosol. The background photocount distribution functions change their parameters and the statistical model, as the spatial position of the recording area in the image plane changes. For these experimental conditions, the spatiotemporal PHDF of the background at the periphery of the studied part of the system's field of view tends to the Bose–Einstein statistics. This creates prerequisites for real time filtering of the scattered background at the synthesis of threshold images.

Acknowledgments

The author is grateful to Yu.V. Gridnev for his help in processing of experimental materials.

References

1. A. Rose, *Vision: Human and Electronic* (Plenum, New York, 1974).
2. B. Crosignani, P. Di Porto, and M. Bertolotti, *Statistical Properties of Scattered Light* (Academic, New York, 1975).
3. V.S. Kozlov, M.V. Panchenko, and A.G. Tumakov, Atmos. Oceanic Opt. **6**, No. 10, 733–738 (1993).
4. B.D. Borisov, V.M. Klimkin, V.A. Krutikov, A.A. Makarov, G.V. Fedotova, and V.A. Chikurov, Atm. Opt. **3**, No. 10, 1003–1007 (1990).
5. V.E. Zuev and M.V. Kabanov, *Transfer of Optical Signals in the Earth's Atmosphere (under Noise Conditions)* (Sov. Radio, Moscow, 1977), 368 pp.
6. G.P. Kokhanenko, Atmos. Oceanic. Opt. **19**, No. 10, 765–772 (2006).